DOI 10.5012/bkcs.2010.31.5.1237

Studies on Morphologies and Mechanical Properties of Multi-walled Carbon Nanotubes/Epoxy Matrix Composites

Min-Kang Seo, Joon-Hyung Byun,† and Soo-Jin Park*

*Department of Chemistry, Inha University, 253, Incheon 402-751, Korea. *E-mail: sjpark@inha.ac.kr*
†Composite Materials Lab, Korea Institute of Machinery & Materials 66 Sangnam-dong, Changwon 641-831, Korea
Received November 16, 2009, Accepted March 8, 2010

The mechanical properties of multiwalled carbon nanotubes (MWNTs)-reinforced epoxy matrix composites with different weight percentages of MWNTs have been investigated. Also, the morphologies and failure behaviors of the composites after mechanical tests are studied by SEM and TEM analyses. As a result, the addition of MWNTs into the epoxy matrix has a remarkable effect on the mechanical properties. And the fracture surfaces of MWNTs/epoxy composites after flexural strength tests show different failure mechanisms for the composites under different nanotube contents. Also, a chemical functionalization of MWNTs can be a useful tool to improve the dispersion of the nanotubes in an epoxy system, resulting in increasing the mechanical properties of the composite materials studied.

Key Words: Composite materials, Failure behaviors, Multiwalled carbon nanotubes, Mechanical properties, Surface properties

Introduction

Recently, extensive research has been carried out on incorporating different types of carbon nanotubes as nano-reinforcements, nano-wires and nano-conductors into polymeric materials to form new composites that possess high mechanical strength, and electrical and thermal conductivity. It has been demonstrated that adding an appropriate amount of nanotubes to polymer-based materials can improve the electrostatic discharge and electromagnetic radio frequency interference protection for space and aircraft applications.[1,2]

In the previous publications, a few researchers have concerned about the relationship between the structural demanding integrity and the interfacial bonding properties in the carbon nanotubes/polymer matrix composites, particularly at extremely low temperature conditions for space applications. However, to successfully achieve outstanding mechanical and electrical performances of these new advanced composite materials, the right understanding of these issues is important.

The interfacial bonding properties and failure mechanisms of carbon nanotubes/polymer matrix composites are important topics that have attracted researchers in recent years.[3,4] Therefore, in this work, we study the effect of carbon nanotube conditions on interfacial bonding properties and failure behaviors of carbon nanotubes/epoxy matrix composites.

Experimental

Materials. Multiwalled carbon nanotubes (MWNTs) used as a reinforcement were manufactured by CVD process (MWNTs were supplied from Iljin Nanotech Co. of Korea, degree of purity: > 90 - 94%, length: 10 - 50 μm, diameter: 10 - 20 nm). The matrix used in this study was an epoxy resin based on diglycidyl ether of bisphenol A (DGEBA, YD-128, Kukdo Chem. Co.), which had an epoxide equivalent weight of 187 $g.eq^{-1}$ and a viscosity of about 5000 cps at 25 °C. Diaminodiphenylmethane (DDM) was selected as a hardener.

Sample preparation. The raw material was first ultra-sonicated and heat-treated to disperse the MWNTs, followed by immersing them in bromine water at 90 °C for 3 h. Then the residual substance was heated in air at 520 °C for 45 min. The black product was soaked in 5 mol/L hydrochloric acid to remove iron particles at room temperature. Finally, the sample was washed with de-ionized water. A 50 wt % yield was obtained after drying in an oven at 150 °C for 12 h.

The epoxy resins were mixed with 0.1, 0.5, 1, and 2 wt % of purified MWNTs. To get a homogeneous mixture, high-energy ultra-sonication was performed for 3 h at 60 °C. Then the curing agent was added to the MWNTs/epoxy and stirred thoroughly. The mixtures were degassed to remove bubbles before casting into a mold. The samples were cured for 2 h at 120 °C, 2 h at 150 °C and 1 h at 200 °C.

Characterizations. The morphology of the specimens was characterized by scanning electron microscopy (SEM, JEOL JSM-840A using 5 keV beam energy) and high-resolution transmission electron microscopy (HRTEM) carried out using an apparatus (JEOL model 2010 TEM using 100 keV beam energy).

The surface of MWNTs/epoxy composite was serially polished through 600 grit silicon dioxide paper, followed by 6, 3, and 1 μm diamond abrasives. A Knoop diamond on a Micromet microhardness tester (Buehler Ltd., USA) was used under a 500 g load. The long diagonal of Knoop indentations was measured in the eye piece of the optical microscope on Micromet microhardness tester at 50X. In this study all materials were measured immediately after indentation. The Knoop hardness was calculated following the equation:[5]

$$KHN = 1.451 \cdot \frac{F}{d^2} \quad (1)$$

where, F is the force in Newton (N) and d is the long diagonal of the Knoop indention in mm.

The mechanical properties of MWNTs/epoxy composites are determined in terms of flexural strength, σ_f and elastic modulus in flexure, E_f. The σ_f and E_f for the specimens determined from three-point bending test are calculated using the following equations:[6]

$$\sigma_f = \frac{3PL}{2bd^2} \tag{2}$$

$$E_f = \frac{L^3}{4bd^3} \cdot \frac{\Delta P}{\Delta m} \tag{3}$$

where, P is the applied load, L the span length, b the width of specimen, d the thickness of specimen, ΔP the change in force in the linear portion of the load-deflection curve, and Δm the change in deflection corresponding to ΔP.

Results and Discussion

Morphologies. Figure 1 presents TEM images of raw MWNTs, purified MWNTs without bromination and purified MWNTs with bromination, respectively. The diameters of the MWNTs are ranged from 5 to 20 nm, as observed by TEM images. The raw MWNTs contains numerous carbon nanotubes, but also a significant amount of iron particles, amorphous carbon and multishell carbon nanocapsules.[7] Figure 1(b) shows that the purity of MWNTs is improved, while some metal particles, amorphous carbon, and multishell carbon nanocapsules are still remained in the sample after purification without bromination. But there is almost no trace of the amorphous carbon, multishell carbon nanocapsules and metal particles in Figure 1 (c), which indicates that the purification with bromination is very efficient.[8]

The pore size distributions of the MWNTs with and without purification are shown in Figure 2. Both specimens show two major peaks around 3 nm and 5 nm, corresponding to the inner-cavity diameter obtained by the TEM image. However the peak of purified specimen is much stronger than that of the raw one, which suggests that the pore area of purified MWNTs increased greatly, attributed to the opened tips of the carbon nanotubes after purification.

Figure 3 (a) shows a plot of the hardness of MWNTs/epoxy composites with different nanotube weight fractions. It is clear that the hardness of the composites with a nanotube weight fraction under 1% is less than that of a pure epoxy sample. However, the hardness is increased by about 20% for a sample with 2 wt % nanotubes. The hardness decrease may be due to the existence of a poor bonding interface between the nanotubes and the matrix.[9,10] However, further increasing the weight fraction of these long nanotubes results in the formation of mesh-like structures, as shown in Figure 3 (b), and these improve the hardness of the composites. Further expatiation, TEM picture of MWNTs/epoxy composites in Figure 3 (c) shows that MWNTs are enveloped with epoxy matrix resins, which is the crosslink chain from reaction between epoxy (on MWNTs' surface) and curing agent. Especially, such envelop structure, in other words, mesh-like structures may provide stronger interfacial adhesion between MWNTs and epoxy matrix in the MWNTs/epoxy composites.

The fracture surfaces of MWNTs/epoxy composites (2 wt % nanotubes) after flexural strength tests show different failure mechanisms for composites pre-treated under different conditions. The tests are conducted immediately at room temperature after removing the composites from the pre-treatment environments. Figures 4 and 5 show the fracture surfaces of the composites pre-treated in warm water (70 ^{o}C) and liquid nitrogen (−180 ^{o}C), respectively. The extreme temperature of −180 ^{o}C is used to simulate a space environment (cryogenic). The fracture process of the 70 ^{o}C heat-treated beam appears to indicate that the failure is the result of a ductile deformation, and nanotubes are aligned perpendicular to the fracture surface, while the fracture of the beam pre-treated in liquid nitrogen is brittle in nature, and nanotubes are aligned parallel to the fracture surface.[9] It is interesting to see in Figure 4 (b) that a nanotube is deformed severely at the tip (a hook-like structure), likely due to breaking of the outer shell of this nanotube. Other nanotubes are in the pullout mode. Figure 5 (b) shows original traces of nanotubes in the composites. These figures show that the fracture process does not follow the nanotube pullout pattern, as shown in Figure 3.

Mechanical properties. Cracks propagate along the plane of the nanotube mesh.[11] Figure 6 shows that the initial flexural stiffness of MWNTs/epoxy composites is greater than that of the composites made using pure epoxy, while the maximum flexural strengths are lower. The maximum flexural strength of the composites pre-treated in liquid nitrogen is greater than that of the

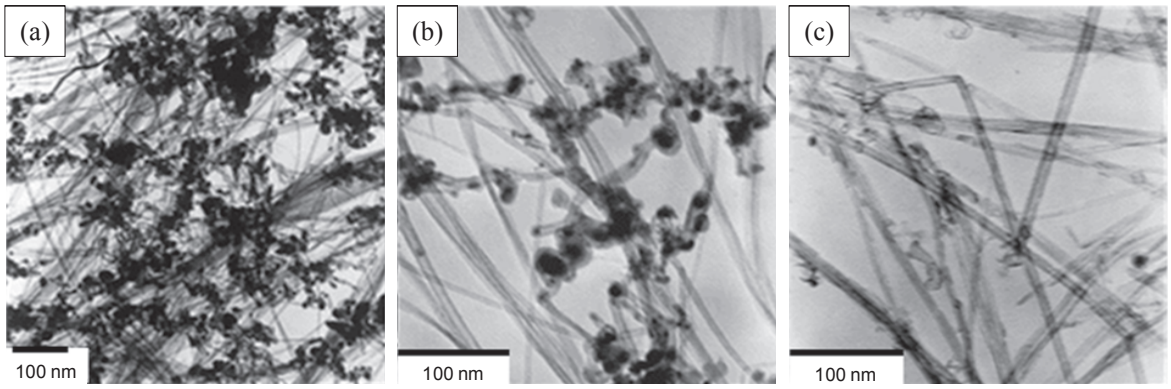

Figure 1. TEM images of (a) the as-received MWNTs, (b) the purified MWNTs without bromination, and (c) the purified MWNTs with bromination.

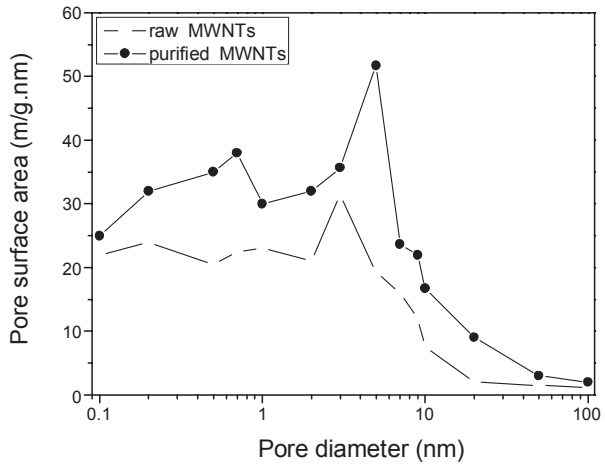

Figure 2. Pore size distribution of MWNTs with and without purification.

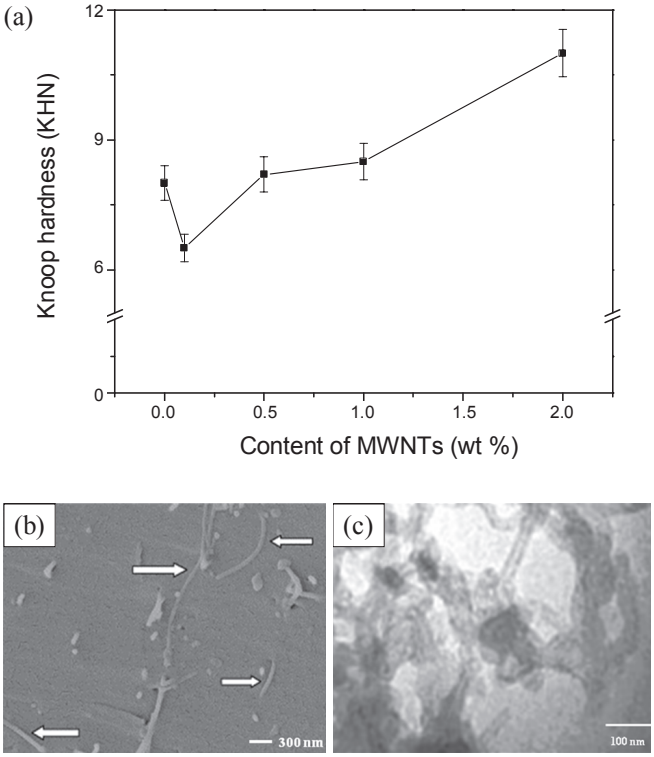

Figure 3. Hardness of MWNTs/epoxy composites with different MWNT contents (wt %) (a) and SEM and TEM pictures of 1 wt % MWNTs/epoxy composites with several long nanotubes (white arrows) linked together to form a mesh-like network structure (b and c).

composites pre-treated in warm water. This may be due to the contraction of the matrix, which increase the clamping stress to the nanotube surface, and thus increase the frictional force between the nanotubes and the matrix. Indeed, the decrease of the flexural strength is not attributed to the strength of the nanotubes since many experimental studies have demonstrated that nanotubes possess superior strength. Therefore, the cause of this strength reduction may be due to the structural non-homogeneity and/or the existence of a weak-bonding interface between the nanotubes and the surrounding matrix.[12,13]

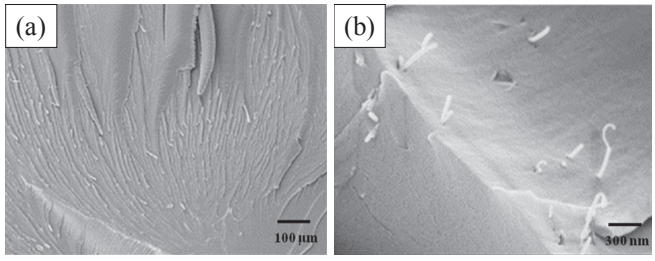

Figure 4. Fracture surfaces of 1 wt % MWNTs/epoxy composites treated in warm water. (a) Fracture takes place in a ductile manner and (b) nanotubes are aligned perpendicular to the fracture surface.

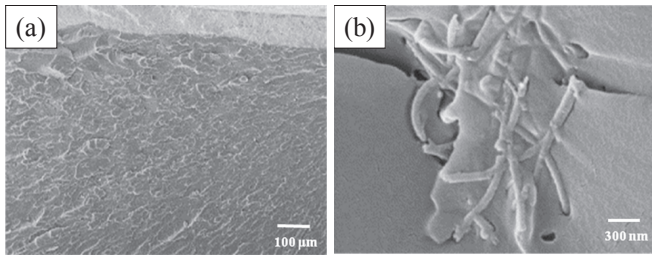

Figure 5. Fracture surfaces of 1 wt % MWNTs/epoxy composites pretreated in liquid nitrogen. (a) Fracture takes place in a brittle manner and (b) the fracture surfaces are parallel to the nanotube mesh.

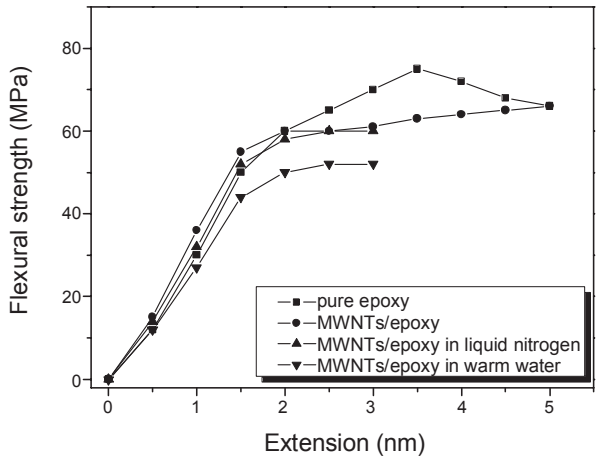

Figure 6. Flexural strength of 1 wt % MWNTs/epoxy composites.

To emphasize the fact that MWNTs can really act as reinforcing materials in composites, we calculated the Young modulus of the catalytic MWNTs from the values obtained for the composites, by using the Cox model.[14] As the real orientation of the nanotubes in the epoxy and the MWNTs length oriented in the stress direction are not known, the parameter η in the Cox model is taken equal to 1. Consequently, for an isotropic composite, its modulus equals:

$$E_x = \frac{1}{6} V_f E_f + V_m E_m \tag{4}$$

By using for the density relation the equation:

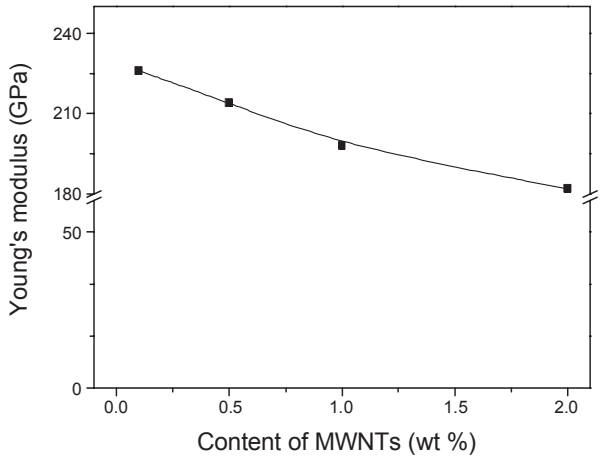

Figure 7. Flexural strength of 1 wt % MWNTs/epoxy composites.

$$\frac{1}{V_f} = 1 + \frac{\rho_f}{\rho_m}\left[\frac{1}{M_f} - 1\right] \quad (5)$$

and considering that for MWNTs ρ_f=2 and for epoxy ρ_m=1.3, we finally obtain:

$$E_f = 6.75\frac{E_x - (1 - V_f)E_m}{V_f} \quad (6)$$

where, E_f is the Young's modulus of MWNTs and E_x the tensile data obtained for the composites.

This relation takes into account the fact that the inner diameter of MWNTs is the third of the outer one, as deduced from HR-TEM characterization.[15,16] The modulus values calculated for the MWNTs from the composites is shown in Figure 7. These by-default values (we supposed an entirely isotropic orientation of MWNTs in the resins) are in the range of those already reported in literature for catalytically grown MWNTs.[17] It is worth noticing that by annealing it is possible to increase intrinsic Young modulus of MWNTs,[18,19] and in that case the composite modulus increases by about 60%.[19]

Consequently, we can indicate that the addition of carbon nanotubes leads to an improvement of mechanical properties for the polymer-based composites and they can form mesh-like structures to reinforce the materials due to the high aspect ratio of the nanotubes.[20] However, these mesh-like structures do not improve the flexural strength because this is mainly determined by the nanotubes/matrix interfacial bonding.

Conclusions

We demonstrated that the microtexture of MWNTs, for equivalent surface chemistry, have an greatly effect on impregnation efficiency and consequently on dispersion of MWNTs in the epoxy matrix resins. Functionalization, either performed by plasma treatment or chemical oxidation, modified surface energy and enhanced wettability and interfacial bonding with epoxy resins. Consequently, the MWNTs were one of the good and appropriate materials to increase elastic behaviors of the composites.

Acknowledgments. This work was supported by Inha University Research Grant.

References

1. Schadler, L. S.; Giannaris, S. C.; Ajayan, P. M. *Appl. Phys. Lett.* **1998**, *73*, 3842.
2. Strong, K. L.; Anderson, D. P.; Lafdi, K.; Kuhn, J. N. *Carbon* **2003**, *41*, 1477.
3. Seo, M. K.; Park, S. J. *Macromol. Mater. Eng.* **2004**, *289*, 368.
4. Seo, M. K.; Lee, J. R.; Park, S. J. *Mater. Sci. Eng. A* **2005**, *404*, 79.
5. Uhl, A.; Michaelis, C.; Mills, R. W.; Jandt, K. D. *Dent. Mater.* **2004**, *20*, 21.
6. Zhou, Y.; Pervin, F.; Lewis, L.; Jeelani, S. *Mater. Sci. Eng. A* **2008**, *475*, 157.
7. Cinke, M.; Li, J.; Chen, B.; Cassell, A.; Delzeit, L.; Han, J.; Meyyappan, M. *Chem. Phys. Lett.* **2002**, *365*, 69.
8. Fan, Y. Y.; Kaufmann, A.; Mukasyan, A.; Varma, A. *Carbon* **2006**, *44*, 2160.
9. Lau, K.T.; Hui, D. *Carbon* **2002**, *40*, 1605.
10. Liu, W.; Zhou, Y. P.; Feng, X. L. *Bull. Korean Chem. Soc.* **2009**, *30*, 3016.
11. Thostenson, E. T.; Chou, T. W. *Carbon* **2006**, *44*, 3022.
12. Seo, M. K.; Park, S. J. *Bull. Korean Chem. Soc.* **2009**, *30*, 124.
13. Shin, J. W.; Jeun, J. P.; Kang, P. H. *J. Ind. Eng. Chem.* **2009**, *15*, 555.
14. Cox, H. L. *Brit. J. Appl. Phys.* **1952**, *3*, 72.
15. Delpeux, S.; Szostak, K.; Frackowiak, E.; Bonnamy, S.; Béguin, F. *J. Nanosci. Nanotechnol.* **2002**, *2*, 481.
16. Colomer, J. F.; Piedigrosso, P.; Willems, I.; Journet, C.; Bernier, P.; Van Tendeloo, G.; Fonseca, A.; Nagy, J. B. *J. Chem. Soc. Faraday Trans.* **1998**, *94*, 3753.
17. Salvetat, J. P.; Bonard, J. M.; Thomson, N. H.; Kulik, A. J.; Forro, L.; Benoit, W.; Zuppiroli, L. *Appl. Phys. A* **1999**, *69*, 255.
18. Pan, Z. W.; Xie, S. S.; Lu, L.; Chang, B. H.; Sun, L. F.; Zhou, W. Y.; Wang, G.; Zhang, D. L. *Appl. Phys. Lett.* **1999**, *74*, 3152.
19. Breton, Y.; Delpeux, S.; Benoit, R.; Salvetat, J.-P.; Sinturel, C.; Béguin, F.; Bonnamy, S.; Désarmot, G.; Boufendi, L. *Molec. Cryst. Liq. Cryst. Sci. Technol. A* **2002**, *387*, 135.
20. Yu, S.; Juay, Y. K.; Young, M. S. *J. Nanosci. Nanotechnol.* **2008**, *8*, 1852.